Very High Frequency Electron Paramagnetic Resonance of 2,2,6,6-Tetramethyl-1-Piperidinyloxy in 1,2-Dipalmitoyl-*sn*-Glycero-3-Phosphatidylcholine Liposomes: Partitioning and Molecular Dynamics

Alex I. Smirnov,* Tatyana I. Smirnova,‡ and Philip D. Morse II§

Illinois EPR Research Center, Departments of *Internal Medicine and ‡Chemistry, University of Illinois at Urbana-Champaign, Urbana, Illinois, and §Department of Chemistry, Illinois State University, Normal, Illinois USA

ABSTRACT Partitioning and molecular dynamics of 2,2,6,6,-tetramethylpiperedine-1-oxyl (TEMPO) nitroxide radicals in large unilamellar liposomes (LUV) composed from 1,2-dipalmitoyl-*sn*-glycero-3-phosphatidylcholine were investigated by using very high frequency electron paramagnetic resonance (EPR) spectroscopy. Experiments carried out at a microwave frequency of 94.3 GHz completely resolved the TEMPO EPR spectrum in the aqueous and hydrocarbon phases. An accurate computer simulation method combined with Levenberg-Marquardt optimization was used to analyze the TEMPO EPR spectra in both phases. Spectral parameters extracted from the simulations gave the actual partitioning of the TEMPO probe between the LUV hydrocarbon and aqueous phases and allowed analysis of picosecond rotational dynamics of the probe in the LUV hydrocarbon phase. In very high frequency EPR experiments, phase transitions in the LUV-TEMPO system were observed as sharp changes in both partitioning and rotational correlation times of the TEMPO probe. The phase transition temperatures (40.5 ± 0.2 and 32.7 ± 0.5°C) are in agreement with previously reported differential scanning microcalorimetry data. Spectral line widths were analyzed by using existing theoretical expressions for motionally narrowed nitroxide spectra. It was found that the motion of the small, nearly spherical, TEMPO probe can be well described by anisotropic Brownian diffusion in isotropic media and is not restricted by the much larger hydrocarbon chains existing in ripple structure ($P_{\beta'}$) or fluid bilayer structure (L_α) phases.

INTRODUCTION

The structure and dynamics of membrane lipids and their relationship to membrane function are important problems in membrane biophysics. Electron paramagnetic resonance (EPR) methods have been applied to membrane studies for over 25 years and have revealed much of what we know about motion (e.g., Polnaszek et al., 1978; Freed, 1987; Dalton and Miller, 1993), order (Seelig, 1970; Costanzo et al., 1994; Morimoto et al., 1994; Crepeau et al., 1994), oxygen permeability (Windrem and Plachy, 1980; Subczynski et al., 1989), and lipid-protein interactions in model and biological membranes (e.g., Schreier et al., 1978; Meirovitch et al., 1984).

Membrane studies by EPR are based on the use of a versatile nitroxide probe. Nitroxides are stable free radicals that have EPR spectra that are sensitive to the molecular microenvironment (fluidity, order, polarity, and pH). Several reviews have described the theory of nitroxide EPR spectral analysis (Nordio, 1976; Schneider and Freed, 1989) and applications of nitroxides to membrane studies (Schreier et al., 1978).

Small nitroxide probes such as 2,2,6,6,-tetramethylpiperedine-1-oxyl (TEMPO; molecular weight 156) partition between the hydrocarbon and aqueous phases of many types of membranes (Linden et al., 1973; Wu and McConnell, 1975). The different values of the TEMPO g-value (**g**) and hyperfine (**A**) tensors in these two phases make it possible to obtain information about the microenviroment of both phases simultaneously.

To date, nitroxide EPR partitioning studies have been carried out at the X-band (microwave frequency band covering the range of 8.8–9.5 GHz used for EPR experiments), where the EPR spectra show a poorly resolved splitting of the high field ($m_I = -1$) nitrogen hyperfine line; the low field ($m_I = 1$) and the mid-field ($m_I = 0$) lines show no resolvable splitting at all. Such spectra are often analyzed in terms of a partition parameter f_X derived from X-band EPR data (Shimshick and McConnell, 1973), which is expressed as the ratio of the least overlapping intensities of the split high field line (we use the subscript X to signify the measurements at X-band). As the nitroxide line width is sensitive to motion of the probe, the temperature dependence of f_X is a combined effect of the partitioning and the changes in the rotational dynamics of the probe, and interpretation of f_X is complicated.

Polnaszek and co-authors (1978) carefully analyzed various factors determining the EPR spectra of spin probes that partition between the aqueous and lipid phases. One approach they employed was based on paramagnetic broadening agents. Paramagnetic broadening agents, such as Ni^{2+} (e.g., Keith and Snipes, 1974) or ferricyanide (e.g., Morse, 1977) are soluble in the aqueous but not in the lipid phase. The presence of a paramagnetic metal ion in the aqueous phase at concentrations of 0.1 M results in broadening beyond detection of the nitroxide EPR signal from this phase. The drawback of this approach is that the high concentrations of paramagnetic metal ions can affect membrane structure and change the thermodynamic properties of the membrane

Received for publication 18 July 1994 and in final form 14 March 1995.

Address reprint requests to Dr. Alex I. Smirnov, Illinois EPR Research Center, University of Illinois, 506 S. Mathews, Urbana, IL 61801. Tel.: 217-244-2252; Fax: 217-333-8868; E-mail: smirnov@b.scs.uiuc.edu.

0006-3495/95/06/2350/11 $2.00

(e.g., Polnaszek et al., 1978, reported a 1°C shift in the temperature of the gel-liquid crystal phase transition when Mg^{2+}, which has a radius similar to Ni^{2+}, was added to the system). It was also suggested that temperature variations in the permeability of the lipid bilayer to Ni^{2+} and/or ferricyanide resulted in some loss of the probe signal from the lipid phase.

In another report, Severcan and Cannistraro (1988) used specially designed deuterated nitroxides (e.g., Plachy and Windrem, 1977), which have approximately 10-fold narrower line width compared with nondeuterated nitroxides (the magnetic moment of the deuterium is much smaller than that of the proton). In a pilot partitioning study using these probes, the splitting of all three nitrogen hyperfine lines was observed. The partitioning coefficients calculated for the $m_I = 0$ (mid-field line) and the $m_I = -1$ (high field line) transitions from the same spectra were different, however. This difference was explained as an effect of molecular motion on the line width, although the actual molar partitioning of the probe between the lipid and aqueous phases was not calculated.

Several attempts have been made to estimate the rotational correlation time of spin probes in membranes from X-band partitioning data and to correlate these estimations with partitioning of the probe (Lee et al., 1974; Polnaczek et. al., 1978; Severcan and Cannistraro, 1988, 1989). Polnaczek and co-authors (1978) derived the rotational correlation time of the probe from the spectra taken with Ni^{2+} ion present in the aqueous phase. They showed that the properties of the membrane are changed by the presence of 0.1 M Ni^{2+}. They suggested that the nitroxide probe TEMPO is preferably distributed near the polar region of the membrane but is in rapid equilibrium with the nitroxide probe distributed throughout the membrane. Severcan and Cannistraro (1988, 1989) obtained better resolved spectra using specially synthesized deuterated probes that permitted the authors to analyze the data in terms of peak-to-peak line width and peak-to-peak height. However, their estimates of the rotational correlation time of the probe in the hydrocarbon region of the membrane are likely to be inaccurate because the magnetic parameters of the probe were not measured. Another source of inaccuracy comes from errors in estimation of the homogeneous line width (no computer modeling was done to calculate the line width). Severcan and Cannistraro also applied the model of an isotropic Brownian diffusion in isotropic media, which is not likely to be applicable to the membrane phase.

It is important to measure accurately the rotational motion of the nitroxide probes in the hydrocarbon region of the membrane. As an example, it was demonstrated by Severcan and Cannistraro (1988) that the tumbling rate of a small nitroxide probe in the lipid phase of lecithin liposomes varies with addition of α-tocopherol. Thus, the EPR dynamics studies of not only traditionally applied lipid-like EPR probes (such as doxyl nitroxide labels) but also relatively small nitroxide molecules (such as TEMPO) can provide additional information about membrane organization, rates of motion of small organic molecules in the membrane phase, and the effects of other molecules on membrane order.

In this paper we demonstrate how very high frequency (VHF; W-band, microwave frequency band covering the range of 94.0–94.3 GHz used for VHF EPR experiments) EPR can be applied not only to derive accurate partitioning data but also to measure the motional parameters of an EPR probe TEMPO in the lipid phase of 1,2-dipalmitoyl-*sn*-glycero-3-phosphatidylcholine (DPPC). The 10-fold increase in g-value resolution at W-band compared with X-band allows us to resolve completely the TEMPO spectrum in both the aqueous and hydrocarbon environments. VHF EPR is especially advantageous in studies of fast molecular motion (Grinberg et al., 1979). The range of detectable correlation times at W-band for a typical nitroxide radical shifts 7-fold toward shorter correlation times (faster motion). Therefore, compared with X-band, the nitroxide spectra at W-band are more sensitive to changes in the tumbling rate and rotational anisotropy of the probe.

The high resolution W-band spectra we obtained were fit by an accurate theoretical model that also accounts for dispersion contributions to EPR signals observed at 94.3 GHz. The spin packet envelope function for TEMPO resulting from unresolved proton superhyperfine and/or inhomogeneities of the magnetic field was assumed to be Gaussian. Inhomogeneously broadened spectra were simulated by using a precision fast convolution algorithm and then optimized by using a Levenberg-Marquardt method (Smirnov and Belford, 1995). As all three nitrogen hyperfine components in both environments are resolved at W-band, a unique solution was obtained with an inhomogeneous lineshape model. Spectral parameters and parameter uncertainties including Lorentzian contributions to line width, and intensities were derived directly from the fitting procedure. This allowed the data to be analyzed by using an anisotropic fast motion model.

MATERIALS AND METHODS

Preparation of lipid vesicles

Large unilamellar liposomes (LUV) were prepared by modification of the method of Mayer et al. (1986). Briefly, 2 ml of DPPC in chloroform (50 mg/ml) was pipetted into a 50-ml round bottom flask, and the chloroform was removed under vacuum (15 mm Hg). The flask containing the dry lipids was then placed on a vacuum line (5 μm Hg) overnight. Phosphate-buffered saline (0.15 M NaCl, 5 mM phosphate buffer, pH 7.0), 0.5 ml, was added to the flask containing the DPPC and swirled in a water bath at 50°C for several minutes. The suspension of lipids was cooled down to 77 K and then placed in the 50°C water bath and swirled again. This freeze-thaw step was repeated 10 times. After the freeze-thaw cycle, the suspension of phospholipids was extruded at 700 lbs/in^2 through two Nucleopore (Nucleopore Corp., Pleasanton, CA) filters with a pore size of 0.1 μm by using a 10-ml extruder (Lipex Biomembranes, Vancouver, British Columbia, Canada) warmed to 50°C. The extrusion process was repeated 10 times to produce the final LUVs. The final concentration of DPPC in aqueous media was 200 mg/ml.

TEMPO (Fig. 1; purchased from Molecular Probes, Eugene, OR) was dissolved in phosphate-buffered saline and added to the LUVs to give a final concentration of 520 μM.

X-band EPR spectroscopy

A Varian (Palo Alto, CA) E-112 spectrometer was equipped with a Varian TE_{102} cavity and a Varian temperature controller (model 906790). The LUV/

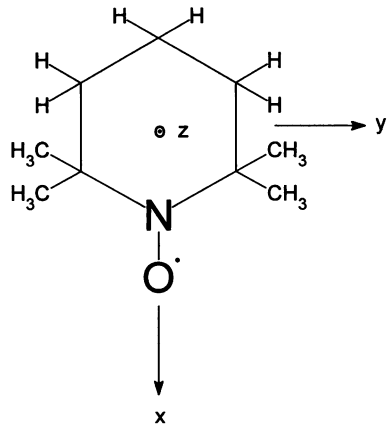

TEMPO

FIGURE 1 Molecular structure of 2,2,6,6-tetramethyl-1-piperidinyloxy (TEMPO) and directions of the magnetic axes (x, y, and z).

TEMPO sample was drawn into a 1-mm internal diameter (i.d.) quartz capillary and subsequently positioned inside the variable temperature dewar insert. The insert was fixed inside the spectrometer cavity. A miniature T-type (copper-constantan) thermocouple (Omega Engineering, Stamford, CT) was attached to the capillary so that its end was just outside the EPR-sensitive region of the cavity. Temperature was measured with an Omega Engineering (model 410A1A) digital temperature indicator. Temperature was stable and reproducible within ±0.2°C; however, because of possible temperature gradients within the dewar insert (Morse et al., 1985; Rothenberger et al., 1993), the accuracy of the temperature over the entire sample was estimated as ±0.5°C. Samples were equilibrated at each temperature for at least 10 min after the temperature reading stabilized. Then, the spectra were continuously recorded until no changes were observed. At each temperature, the last recorded spectrum was used for further analyses.

An IBM personal computer with an IBM analog-digital card and a commercial EPR software package (Scientific Software Services, Bloomington, IL) was used for data acquisition.

W-band EPR spectroscopy

The W-band (94 GHz) EPR spectrometer constructed at the University of Illinois EPR Research Center was described elsewhere (Wang et al., 1994). The magnetic field was supplied by a Varian XL-200 superconductive magnet set to 33,601.8 G. The magnetic field was scanned (within ±150 G; variable offset) with a room temperature air-cooled solenoid coil placed inside the room temperature bore of the magnet. A Varactor-tuned Gunn oscillator (ZAX Millimeter Wave Corp., San Dimas, CA) with a 35-mW power output at 94.3 GHz was used as a microwave source. The cavity was a cylindrical type TE_{01n} (n = 2 or 3, depending on tuning) resonator fabricated from the machinable ceramic MACOR (Corning Glass, Corning, NY) with a fired-on gold surface. The quality factor of the unloaded cavity was 4000. The cavity was fixed inside a brass waveguide block that provided excellent mechanical and thermal stability. A tunable Shottky diode (Hughes Aircraft Co., Microwave Products Division, Torrance, CA) with a low noise preamplifier and bias current supply was used for microwave detection. Phase-sensitive detection at a magnetic field modulation of 100 kHz was provided by a SR-530 lock-in amplifier (Stanford Research Systems, Sunnyvale, CA).

The magnetic field was calibrated by using a high precision NMR teslameter (Metrolab PT 2025, GMW Associates, Redwood City, CA). The homogeneity of the field over the sample region was estimated to be better than 20 mG. The microwave frequency was measured with an EIP 578 in-line microwave frequency counter (EIP Microwave, San Jose, CA). Sample temperature was monitored by using two Fluke digital thermometers (Model 51, Fluke, Palatine, IL) equipped with K-type (aluminum-nickel alloy) miniature thermocouples fixed inside the upper and lower parts of the microwave cavity block. For low temperature experiments, nitrogen gas was passed through a heat exchanger immersed into liquid nitrogen and then through a foam-insulated line into the bore of the superconductive magnet to cool the entire cavity assembly. For measurements above room temperature, we used a simple apparatus constructed from an Escort (Ronson Corp., Somerset, NJ) household hair dryer powered through a Variac (General Radio Company, Concord, MA) autotransformer. Air flow from the hair dryer was directed into the bore of the magnet to the cavity assembly. By varying the Variac output voltage, we were able to vary the cavity temperature. The temperature of the air exiting the hair dryer was monitored by an additional thermocouple. The massive microwave block provided uniform temperature throughout the cavity. Temperature was considered stable when, within the time of the EPR measurement, readings of both thermometers remained the same within ±0.1°C. EPR spectra were taken until both temperature and spectra were stable, and the last spectrum in the set was used for further analyses.

The LUV/TEMPO sample was drawn into a quartz capillary (i.d. = 0.15 mm, outside diameter = 0.25 mm; Vitro Dynamics, Rockaway, NJ) that was placed inside the W-band resonator. The capillary was coaxial to the cavity and did not decrease significantly the resonator quality factor. To avoid possible distortion of the narrow EPR signals by the automatic frequency control system, the automatic frequency control circuit was switched off (Smirnov et al., 1994) after careful tuning, and the frequency was monitored with the EIP 578 microwave counter. In this mode, the stability of the microwave frequency was better than 1 ppm during the time of the measurement (1 min). Other typical spectrometer settings were as follows: modu-

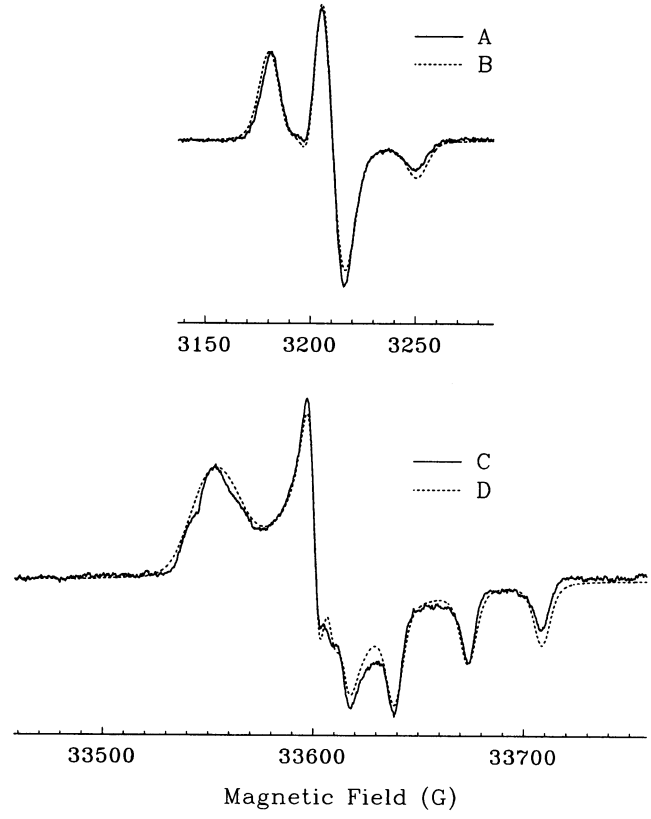

FIGURE 2 Rigid limit EPR spectra of TEMPO in a 2:1 (v/v) mixture of oleic acid and canola oil at 9.0 GHz (A, solid line, T = −150°C) and 94.3 GHz (C, solid line, T = −135°C). Corresponding least-squares simulations are shown in dashed lines and are described in the text. Magnetic parameters are given in Table 1.

lation amplitude, 0.1 G; microwave attenuation, 10 dB; scan width, 100.7 G; and number of data points, 2048.

Measurements of magnetic tensors

As stated above, high frequency EPR spectroscopy is advantageous for studying solvent effects on both **g** and hyperfine **A** tensors of nitroxide radicals (Ondar et al., 1985). The magnetic parameters (g and A tensors) of TEMPO in lipids were estimated by using a 0.4 mM TEMPO solution in a mixture (2:1, v/v) of oleic acid (purchased from Aldrich Chemical Co., Milwaukee, WI) and canola oil (purchased from a local supermarket). Oleic acid was chosen to mimic the membrane hydrocarbon region. The oleic acid alone freezes to a polycrystalline phase; after addition of canola oil to the oleic acid, the formation of a glass was observed upon freezing.

Components of the magnetic tensors were measured at 94.3 GHz (T = −135°C), where the TEMPO spectrum is near its rigid limit (Fig. 2*C*). The spectrum was simulated by using the HPOW program (Illinois EPR Research Center). Anisotropic line width was adjusted by using the SIMPLEX optimization procedure as were the canonical components of the **g** and **A** tensors. A nonadjustable 6° angle between the **A** and **g** tensors in the *x-y* plane (e.g., see Schreier et al., 1978) was included in the simulation. Best least-squares fit of the data is shown in Fig. 2*D*.

The value of A_x is difficult to measure directly from the experimental 94.3-GHz spectrum as the corresponding lines are poorly resolved as a result of unresolved proton superhyperfine and/or g-strain broadening at this frequency. At lower frequencies (e.g., X-band) g-strain should be negligible. To check the consistency of the simulation, we measured the rigid limit spectrum (T = −150°C) for the same TEMPO-lipid/oil system at X-band (Fig. 2*A*) and repeated the simulation adjusting only the line widths and the isotropic g-value; the g-anisotropy and the canonical components of the **A** tensor were the same as from the W-band fit. The isotropic g-value was adjusted over a small range (corresponding to <1 G at X-band) to account for differences in magnetic field calibration between the two spectrometers. The result of the fit (Fig. 2*B*) demonstrates that our simulations at both W- and X-band are consistent. Full optimization of parameters for the X-band spectrum improved the residual norm insignificantly (<5%).

Magnetic parameters extracted from the 94.3-GHz spectra (see Table 1) are compared with those reported for a TEMPO toluene glass (Ondar et al., 1985) measured at 148 GHz (the magnetic parameter for lipid-like solvents were not reported by Ondar et al., 1985). Some differences between the absolute values of the **g** and **A** tensors in our work and that of Ondar et al. can be explained by the slightly different polarity of the solvents as well as by different calibration of the magnetic fields and a small uncorrected dispersion contribution present in the spectra at 148 GHz.

TABLE 1 Magnetic parameters of TEMPO in hydrophobic solvents

	94.3 GHz	148 GHz
g_x	$2.00955 \pm 5 \times 10^{-5}$	$2.00980 \pm 7 \times 10^{-5}$
g_y	$2.00632 \pm 5 \times 10^{-5}$	$2.00622 \pm 7 \times 10^{-5}$
g_z	$2.00240 \pm 5 \times 10^{-5}$	$2.00220 \pm 7 \times 10^{-5}$
$\langle g \rangle$	$2.00609 \pm 9 \times 10^{-5}$	$2.00607 \pm 1.2 \times 10^{-4}$
g_{iso}	$2.00616 \pm 4 \times 10^{-5}$	$2.00611 \pm 4 \times 10^{-5}$
A_x/γ_e	6.84 ± 0.50	6.0 ± 0.1
A_y/γ_e	6.84 ± 0.20	7.3 ± 0.1
A_z/γ_e	35.0 ± 0.2	34.2 ± 0.3
$\langle A \rangle/\gamma_e$	16.2 ± 0.6	15.8 ± 0.3
a_{iso}	16.38 ± 0.02	15.5 ± 0.2

The 94.3 GHz data are from this work; parameters for TEMPO in 2:1 (v/v) mixture of oleic acid and canola oil determined by spectral simulation. The 148-GHz data are from Ondar et al. (1985); parameters of TEMPO in toluene determined from spectrum without simulation.
$\langle g \rangle = (g_x + g_y + g_x)/3$; g_{iso} and a_{iso} measured from EPR spectra in fast motion limit; $\langle A \rangle = (A_x + A_y + A_z)/3$. The errors in magnetic parameters are mainly determined by errors in magnetic field calibration. γ_e is the magnetogyric ratio of the free electron.

RESULTS AND DISCUSSION

ANALYSIS OF EXPERIMENTAL DATA AT 9.0 AND 94.3 GHZ

A typical X-band (9.2 GHz) EPR experimental spectrum for DPPC LUV/TEMPO is shown in Fig. 3*A* (T = 37.6°C). The partition parameter f_x at this frequency is usually defined as:

$$f_x = H/(H + P) \quad (1)$$

where H and P are as shown in Fig. 3*A*. It was assumed (e.g., Shimshick and McConnell, 1973) that f_x is approximately equal to the fraction of spin label dissolved in the membrane bilayer.

A high frequency (W-band, 94.3 GHz) EPR spectrum for the DPPC LUV/TEMPO system at the same temperature (37.6°C) is shown in Fig. 3*B*. Three intense lines of approximately equal peak-to-peak line width (Fig. 3*B*, spectrum 1) correspond to the TEMPO molecules in the aqueous environment. All three lines of the hydrocarbon TEMPO EPR spectrum (spectrum 2) are clearly resolved and shifted down field because of the higher value of g_{iso} in the hydrocarbon phase compared with g_{iso} in the aqueous phase.

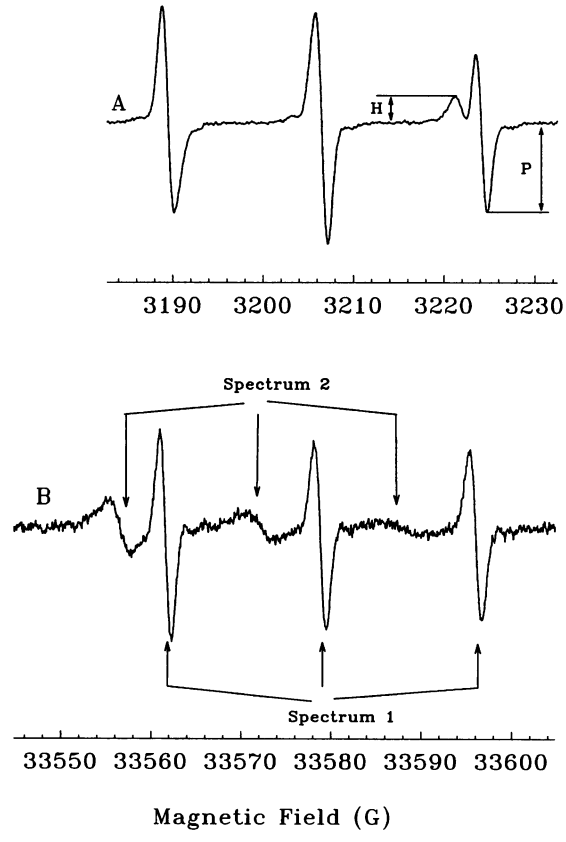

FIGURE 3 Experimental EPR spectra at 37.6°C of DPPC LUV and TEMPO at 9.0 (*A*) and 94.3 GHz (*B*). The amplitudes of the split high field nitrogen hyperfine component in (*A*) are used to calculate the X-band (9.0 GHz) partitioning coefficient $f_x = H/(H + P)$. In contrast to (*A*), the 94.3-GHz experiment (*B*) completely resolves the spectra arising from TEMPO molecules in the aqueous phase (spectrum 1) and the hydrocarbon phase (spectrum 2).

To obtain rotational motion and partitioning information from these spectra, we extended our software (Smirnov and Belford, 1995) to simulate two overlapping nitroxide spectra in the fast motion limit. A fast convolution algorithm was used to precisely simulate inhomogeneously broadened nitroxide spectra. Unresolved proton superhyperfine structure was modeled by a Gaussian envelope function. Different isotropic values of **g** and **A**, g_{iso} and A_{iso}, and the Gaussian envelopes ($\Delta B^{G}_{p\text{-}p}$) were assigned for the aqueous and hydrocarbon membrane environments. The dispersion contribution (or microwave phase shift) was assumed to be the same for both components of the TEMPO signal. This microwave phase shift was usually present in the VHF EPR spectra and was different from tuning to tuning and sample to sample. The baseline was modeled as a linear function. During least-squares Levenberg-Marquardt optimization, the following parameters were allowed to vary: isotropic values of **g** and **A**, g_{iso} and A_{iso} (different for aqueous and hydrocarbon membrane phases), the inhomogeneous broadening parameter $\Delta B^{G}_{p\text{-}p}$ (different for each of the phases), homogeneous line width $\Delta B^{L}_{p\text{-}p}(m_I)$ (different for each of the nitrogen hyperfine components $m_I = 1, 0, -1$ and for each of the phases), intensities of the signal in the phospholipid and aqueous phases, microwave phase shift (or weight of the dispersion contribution), and the coefficients of the linear baseline. Small satellite lines usually observable in the spectrum because of the small natural abundance of ^{13}C isotope were also included in the simulations of the spectra with a high signal-to-noise ratio. We also noticed that, when the experimental amplitude of the satellite ^{13}C transitions was comparable with the standard deviation of the noise, introducing the satellites into the fitting procedure did not change the fitting results. The Levenberg-Marquardt algorithm also allowed us to conveniently fix any of the adjustable parameters for least-squares optimization.

All fitting parameters, including Lorentzian and Gaussian components of the line width, were extracted directly from the fit. The spectral intensity of TEMPO in the aqueous and hydrocarbon phases were also obtained directly from the fit. This further improved the accuracy of calculated partitioning. Usually, intensities of the EPR signals are determined from peak height/line width measurements or after digital double integration of the spectra. Both methods can be inaccurate in the case of inhomogeneously broadened lines. For example, it is known that digital integration of inhomogeneously broadened EPR lines is inaccurate because of the broad wings of the Lorentzian function. The Lorentzian function integrated over a spectral window of 5 line widths is only $\approx$89% of the integral calculated over a spectral window of 50 line widths; such spectral windows are not always possible in the experiment. The commonly used estimation of intensity as a product of line height and line width squared is valid only for the same ratio of $\Delta B^{G}_{p\text{-}p}$ to $\Delta B^{L}_{p\text{-}p}$ (for inhomogeneously broadened lines) and cannot be used if this ratio is varied during the experiment (e.g., $\Delta B^{L}_{p\text{-}p}$ is varied with the temperature).

Initial simulation parameters are entered by the operator during the interactive menu dialogue and then the iterations are started. The iterations are stopped after the value of χ^2 is improved insignificantly (i.e., by 10^{-3} of the previous value) for a second time. In most cases, the algorithm converged in only five to seven iterations. The estimates of parameter uncertainties were calculated in a standard manner (given as 68% confidence intervals) with a covariance matrix (Press et al., 1986; Halpern et al., 1993). In EPR partitioning experiments, the spectra gradually change with the temperature. Therefore, the spectra can be processed in sequence; the best fit for one spectrum can be used as a first approximation for the next spectrum. Most of the W-band spectra were processed in such a sequential automatic mode without any intervention from the operator.

Fig. 4 demonstrates the ability of the fitting procedure to extract the aqueous (*C*) and the hydrocarbon (*B*) spectra from the experimental spectrum (*A*) taken at T = 38.3°C, which is below the main phase transition of the DPPC LUV. The residual (Fig. 4*D*), which is the difference between the experimental spectrum and the simulation, shows no systematic deviation between the experiment and the fit. The standard deviation of the residual corresponds to that of spectrometer noise. After fitting, the hydrocarbon and aqueous phase spectra were simulated by using all best-fit parameters except the microwave phase shift, which was set to zero (Fig.

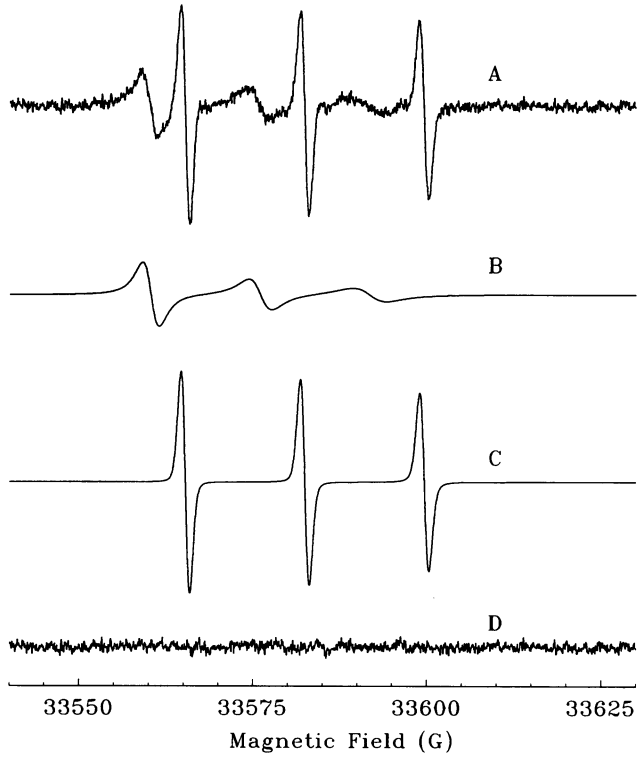

FIGURE 4 Experimental and simulated 94.3-GHz EPR spectrum of DPPC LUV and TEMPO at 38.3°C (below the main phase transition). Simulated and experimental spectra are essentially identical (*A*). (*D*) is the residual. The simulated EPR spectra of the TEMPO probe in the hydrocarbon (*B*) and aqueous (*C*) phases are shown after correction for the microwave phase shift observed at 94.3 GHz.

4, *B* and *C*). The spectrum shown in Fig. 5*A* was taken at T = 42.8°C, which is above the main phase transition; the spectra in Fig. 5, *B*, *C*, and *D*, were defined as in Fig. 4.

We paid special attention to the uniqueness of the fit. The iterations were started from different initial parameter values (e.g., different $\Delta B^{G}_{p\text{-}p}$ and $\Delta B^{L}_{p\text{-}p}(m_I)$ to insure that the global χ^2 minimum was achieved. It was found that the high spectral resolution achieved at 94.3 GHz provided a stable solution; all iterations converged to the global minimum (for a further discussion of fitting well resolved inhomogeneously broadened lines, see Halpern et al., 1993, and Smirnov and Belford, 1995). When the same simulation approach was applied to X-band spectra, we found that the solution was not unique using our model. An example of an X-band spectrum taken at 43°C is shown in Fig. 6. Although the residual (Fig. 6*D*) reveals no systematic deviations between the fit and experiment, the extracted TEMPO aqueous signal (Fig. 6*C*) is in disagreement with motion narrowing theory (the high field line is the narrowest). We also found other minima that described the experimental spectrum quite well (within 0.5% of χ^2_{min}), including one with almost equal nitrogen hyperfine components of the TEMPO aqueous signal. This demonstrates that good resolution between the spectral lines as obtained for the DPPC/TEMPO system at W-band is an important condition for the uniqueness of the fit.

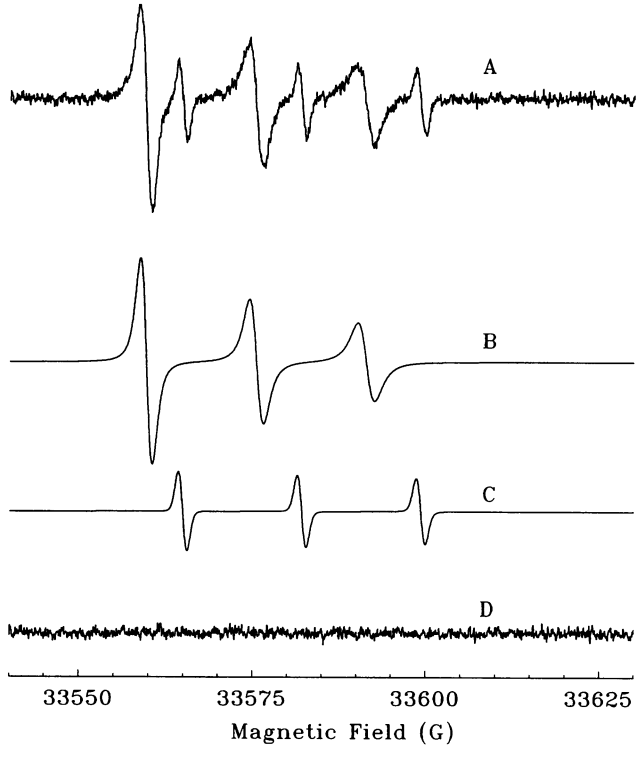

FIGURE 5 Experimental and simulated 94.3-GHz EPR spectra of DPPC LUV and TEMPO at 42.8°C (above the main phase transition). Simulated and experimental spectra are essentially identical (*A*). The residual (*D*) shows no systematic deviations of the fit from the experimental spectrum. The simulated EPR spectra of the TEMPO probe in the hydrocarbon (*B*) and aqueous (*C*) phases are shown after correction for the microwave phase shift.

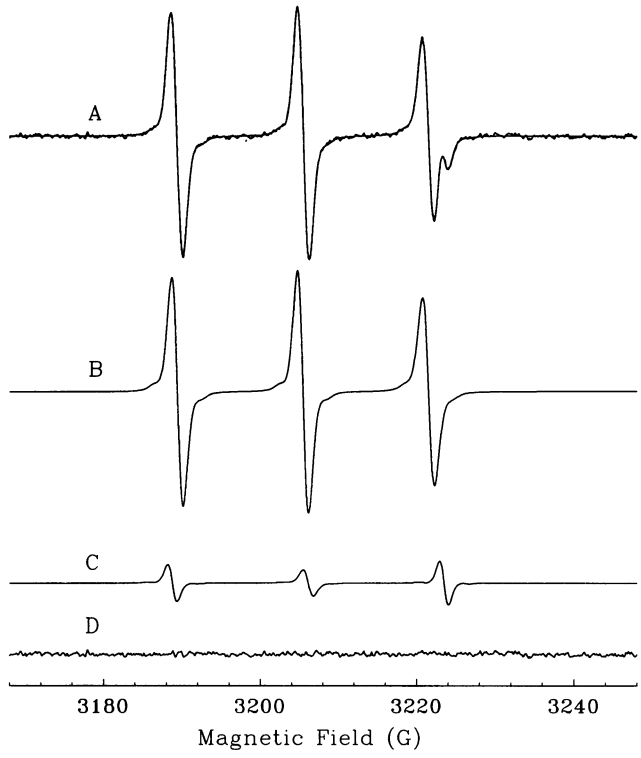

FIGURE 6 Experimental and one of the best-fit simulated 9.0-GHz (X-band) EPR spectra of DPPC LUV and TEMPO at 43.8°C (above the main phase transition). Simulated and experimental spectra are essentially identical (*A*). The residual (*D*) shows no systematic deviations of the fit from the experimental spectrum. The spectra in the hydrocarbon phase and aqueous phases are shown as (*B*) and (*C*), respectively. Because at this frequency the fit is not unique, this particular solution gives the wrong spectrum of TEMPO in the aqueous phase (*C*).

Partitioning of TEMPO between the hydrocarbon and aqueous phases

W-band (94.3 GHz) spectra from TEMPO partitioned between both hydrocarbon and aqueous membrane phases were collected between 20°C and 50°C. Intensities of the TEMPO signal from the hydrocarbon ($I(H)$) and the aqueous ($I(P)$) phases were obtained directly from the fit, and their ratios $f_W = I(H)/I(P)$ are shown in Fig. 7 (filled circles). Error bars correspond to 68% confidence intervals. The parameter f_W gives the actual molar partitioning of the probe and is not derived from the relative intensities of the nitrogen hyperfine components as is parameter f_X (Eq. 1).

The f_W data show two abrupt transitions. The first transition at T = 40.5°C corresponds to a ripple structure ($P_{\beta'}$)-fluid bilayer structure (L_α) phase transition, and the temperature we measured is in agreement with other EPR studies (Shimshick and McConnell, 1973; Wang et al., 1993). The second transition at T = 32.7°C corresponds to the gel structure ($L_{\beta'}$)-ripple structure ($P_{\beta'}$) phase transition (or pretransition). The temperature of this phase transition has been verified previously by diverse physical techniques, e.g., see Chen and Sturtevant (1981). The observed temperature of the $L_{\beta'}$-$P_{\beta'}$ phase transition (32.7°C) from the W-band data is close to the temperature obtained from calorimetric data

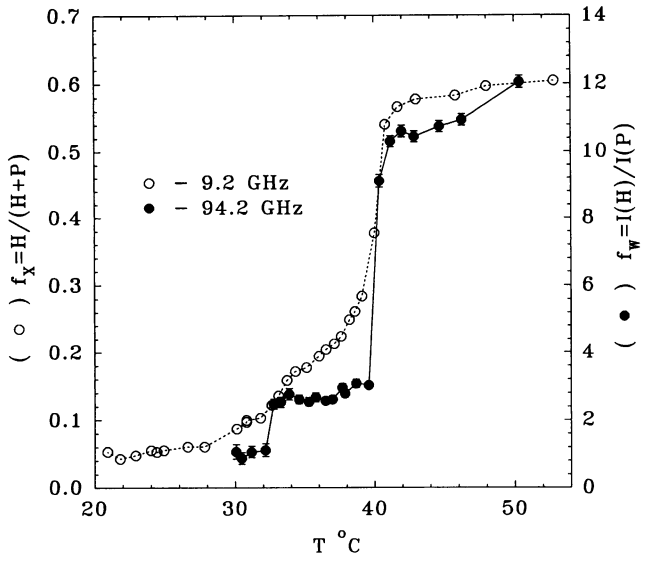

FIGURE 7 Temperature dependence of the TEMPO partitioning parameter f_X (○) calculated from X-band data compared with f_W (●) derived by computer simulations from W-band spectra.

(midpoint T = 34.8°C, (Chen and Sturtevant, 1981)) and X-band EPR data (midpoint T ≈34°C, Wang et al., 1993; some differences in the reported pretransition temperature could be explained by different LUV preparation procedures). According to the W-band data (parameter f_W), the changes in the TEMPO partitioning at the pretransition occur within a temperature interval of 0.6°C, which is much smaller than was previously reported (at least 2°C; Wang et al., 1993).

Although the W-band spectra were collected between 20°C and 50°C, we were unable, at the current signal-to-noise ratio, to extract that part of the spectrum corresponding to the hydrocarbon environment at T < 30°C (below 30°C, the estimated uncertainties in intensity and line width were between 50 and 100%). This indicates a change in the TEMPO spectrum arising from the phospholipid phase most likely because of a further decrease of the TEMPO tumbling rate in the phospholipid environment.

For comparison, we collected X-band spectra from the same system (using a larger sample) at X-band and measured the parameter f_X (Eq. 1). The temperature dependence of f_X observed in our X-band experiments (Fig. 7, open circles) is very similar to data from the literature (Shimshick and McConnell, 1973). Below the $(P_{\beta'})$-(L_α) phase transition at approximately 40.5°C, the parameter f_X undergoes a gradual change and then, after a second transition occurring at 29°C < T < 30°C, stabilizes at the value $f_X \approx 0.05$. The second transition is hardly noticeable on the f_X versus T plot and is much broader than the main phase transition.

Our data show that the high spectral resolution obtained at 94.3 GHz simplifies measurement of the partitioning even for nondeuterated probes such as TEMPO, for which interpretation of the X-band data is complicated by effects of rotational motion on the probe signal arising from the hydrocarbon phase, as was also pointed out by Severcan and Cannistraro, (1988, 1989).

Spectral subtraction is an alternative approach to obtain the molar partition coefficients. Wang and co-authors (1993) used this technique to measure TEMPO partitioning in DPPC liposome aqueous dispersions at X-band. The method is based on recording high field nitrogen hyperfine components ($m_I = -1$) of EPR spectra from a TEMPO aqueous solution and a TEMPO-labeled DPPC dispersion in separate experiments. These spectra were subtracted from each other to yield the component of the TEMPO EPR spectrum in the lipid phase. As the intensity of the TEMPO signal in the aqueous phase of the DPPC dispersion is not known a priori, it has to be adjusted before the spectral subtraction , as does the field position in some cases (e.g., if the g-value was not measured with enough accuracy). Unfortunately, Wang et al. did not describe any criteria for such adjustments. One possibility was that the subtraction was done to obtain a look-alike TEMPO phospholipid signal, which may lead to some uncontrolled errors.

The method of spectral fitting described here uses the standard least-squares criterium for fitting both aqueous and phospholipid TEMPO signals and therefore seems to be more accurate than spectral subtraction. Moreover, the use of the Levenberg-Marquardt algorithm allowed us to estimate the parameter errors for the W-band experiment; as described in the previous section, at X-band, the fitting solution may not be unique. When the number of fitting parameters at X-band was reduced (e.g., for aqueous TEMPO signal, the unresolved proton superhyperfine and the tumbling rate can be measured from a separate experiment), a unique fitting solution may be obtained. This will be discussed further in the next section.

Overall, the high resolution studies of EPR probe partitioning in the lipid dispersions at 95 GHz may be advantageous inasmuch as, compared with X-band, a separate set of data for the aqueous nitroxide signal is not required.

Rotational diffusion of TEMPO in the hydrocarbon phase

The phospholipids that comprise the DPPC LUV at temperatures above the pretransition are microscopically ordered whereas the whole sample is macroscopically disordered. The EPR spectra in such systems (referred to as microscopically ordered but macroscopically disordered) for some nitroxide spin labels were discussed by Meirovitch and Freed (1980a,b), Meirovitch et al. (1984), and Ge and Freed (1993). Using well-oriented and low water content (2–15 wt%) bilayers, Meirovitch and Freed (1980a,b) have shown that perdeuterated TEMPONE (2,2′,6,6′-tetramethyl-4-piperidine-1-oxyl; a nitroxide probe similar to the TEMPO used in this work) exhibits a small but nonnegligible ordering in the fluid hydrocarbon phase of the phospholipid bilayer (L_α).

Microscopic ordering of the nitroxide probe is likely to depend upon the probe location relative to the hydrocarbon chain. Polnaszek et al. (1978) suggested that TEMPO dis-

tributes throughout DPPC membranes and diffuses rapidly within the membrane in the fluid phase. In the presence of paramagnetic broadening agents, they also observed a disappearance of approximately 75% of the signal expected for TEMPO in the lipid phase and concluded that most of this radical is located very close to the aqueous phase (i.e., in the polar head region). At high water concentrations (80 wt% in this work), water molecules may significantly penetrate into the fluid membrane bilayer and introduce additional disorder within the polar head group compared with a low water content membrane studied by Meirovitch and Freed (1980a,b). Therefore, one may expect that ordering effects on the TEMPO spectrum in the L_α phase are likely to be small.

The ordering effect for a fast tumbling nitroxide will alter the spectrum by (1) introducing additional inhomogeneous broadening (most likely to be different for different nitrogen hyperfine components), (2) altering the symmetry of the lines, and (3) altering the observed homogeneous line width from those corresponding to nonrestricted motion. The 94.3-GHz spectra were checked for these specific effects. No additional inhomogeneous broadening was observed. As is shown in Figs. 4 and 5, the data can be fitted to an inhomogeneous lineshape model with the same Gaussian width for all three nitrogen hyperfine components; the residuals revealed no systematic deviations between the experiment and the fit. Also, it was found that the ratios of Gaussian line widths corresponding to the TEMPO lipid signal to those arising from the aqueous phase were approximately 0.92. This value is in agreement with the ratio of the corresponding nitrogen hyperfine constants, 0.925 (the main origin of TEMPO inhomogeneous width is unresolved proton superhyperfine, which, as well as nitrogen hyperfine, should scale approximately with polarity of the microenvironment). Although the spectra shown in Figs. 5 and 6 are not symmetric, the asymmetry is explained not by the ordering effect but by the presence of a dispersion contribution that was found to be the same for both lipid and aqueous signals.

The temperature variation of the homogeneous (Lorentzian) peak-to-peak line widths corresponding to the TEMPO W-band spectrum in the hydrocarbon phase is shown in Fig. 8. Line widths of all three nitrogen hyperfine components (listed according to nuclear quantum number m_I) undergo abrupt changes at the temperatures corresponding to the $L_{\beta'}$-P_β and $P_{\beta'}$-L_α phase transitions. Fig. 8 shows that below the $L_{\beta'}$-P_β phase transition temperature the motion of the probe falls into an intermediate region (i.e., cannot be considered within the fast motion limit) whereas at temperatures above this phase transition the fast motion limit can be applied.

In the fast tumbling limit, the homogeneous line width (T_2^{-1}) of an individual hyperfine line is given (e.g., Nordio 1976) by:

$$T_2^{-1}(m_I) = A + B\,m_I + C\,m_I^2 \qquad (2)$$

where m_I is the z component of the nitrogen nuclear spin quantum number, and A, B, and C are line width parameters that can be expressed in terms of spectral densities or magnetic parameters and a rotational diffusion tensor (Freed, 1964). Recently, the theoretical expressions for motionally narrowed nitroxide line widths and fully anisotropic Brownian diffusion have been modified appropriately for the high field case (Budil et al., 1993). We have used theoretical results from Budil et al. (1993) to analyze the rotational motion of TEMPO in the membrane phase of the DPPC LUVs.

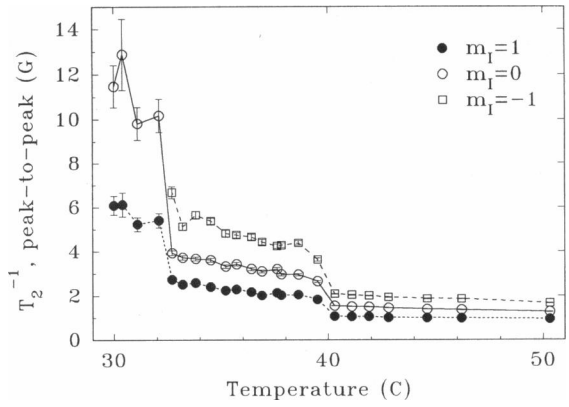

FIGURE 8 Temperature dependence of the homogeneous (Lorentzian) peak-to-peak line width for spectra of TEMPO in the hydrocarbon phase extracted from 94.3 GHz (W-band) experiments. Nitrogen hyperfine components are numbered according nuclear quantum number m_I.

Line width parameters A and B were determined from the experimental spectra at T > 32.5°C and are shown in Fig. 9. At 94.3 GHz, the relative uncertainties in C were found to be much larger than for A or B (the contributions from A and B dominate the overall line width); therefore C was excluded from our analysis. Both A and B parameters undergo a sharp change at the temperature corresponding to the $L_{\beta'}$-P_β phase transition, which is an indication of a change in mobility of the probe between the $L_{\beta'}$ and P_β phases.

As was shown by Budil et al. (1993), the A/B ratio is a key constraint in determining rotational anisotropy from VHF

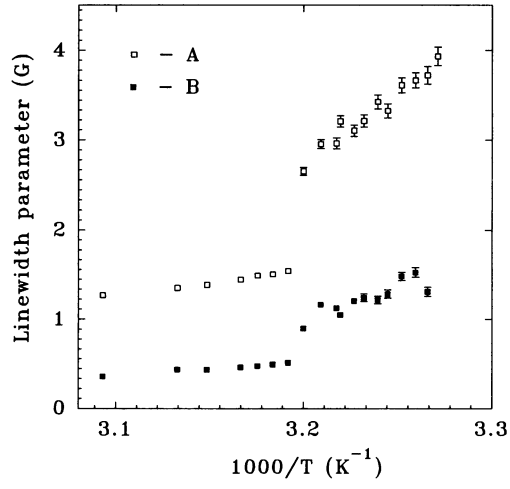

FIGURE 9 Fast motional line width parameters (A and B) for TEMPO in the hydrocarbon phase of DPPC LUV measured at 94.3 GHz as a function of temperature.

EPR data. When nonsecular spectral densities are neglected but secular/pseudosecular reduced spectral densities are retained, then the A, B, and C spectral parameters are proportional to the rotational correlation time τ_R. Therefore the ratio A/B is a constant and is related to the anisotropy of the rotational diffusion tensor by the allowed value equation (AVE):

$$\rho_x = \alpha\rho_y + \beta, \quad (3)$$

where $\rho_x = R_x/R_z$, $\rho_y = R_y/R_z$; R_i are the principal values of the diffusion tensor $\mathbf{R}$, and constants α and β are the functions of A/B ratio, principal values of $\mathbf{g}$- and $\mathbf{A}$-tensors, and the magnetic field as described by Budil et al. (1993).

A plot of parameter A versus B in the temperature range 32.5°C < T < 51.0°C is shown in Fig. 10. One group of experimental data points (with smaller A and B values) corresponds to temperatures above the main phase transition. Another group (with larger A and B values) corresponds to the ripple structure phase of the membrane. Although the two groups of data points are separated, they fall on the same straight line. The slope of the line is $A/B = 2.27 \pm 0.1$ with the intersect $A' = 0.43 \pm 0.09$ G. In our experiments, the main contribution to A′ was broadening from molecular oxygen that was not removed from the sample. This broadening is proportional to the average oxygen permeability of the DPPC liposomes $P = D \times S$, where D is the oxygen diffusion coefficient and S is the oxygen solubility. Windrem and Plachy (1980) have studied how the coefficient P is affected by temperature and/or probe position in the DPPC lipid bilayer using perdeuterated di(*t*-butyl)nitroxide. They found that, at T ≈50°C (above the main phase transition), 1.4×10^{-6} cm^{-2} s^{-1} < P < 2.4×10^{-6} cm^{-2} s^{-1}, depending on the position of the spin label on the carbon chain. This interval corresponds to a range of 0.25–0.44 G for line width broadening $\delta(\Delta B_{p\text{-}p})$ when expressed as peak-to-peak line width. These values bracket the non-zero intersect A' observed from our A-B plot.

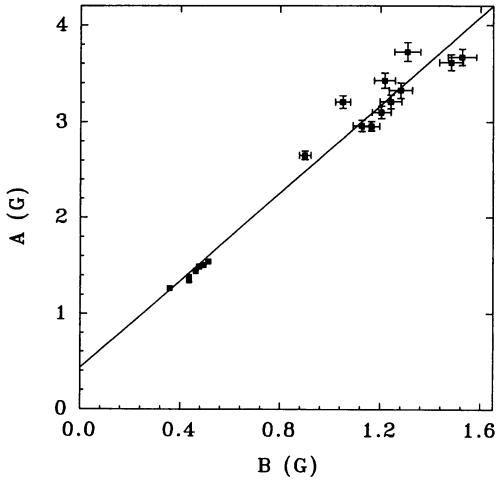

FIGURE 10 A versus B line width parameters measured at 94.2 GHz for TEMPO in the hydrocarbon phase of DPPC LUV over the temperature range 33–51°C. The solid line is the least-squares fit with slope $A/B = 2.27 \pm 0.1$ and intersect $A' = 0.43 \pm 0.09$ G.

Oxygen permeability of the DPPC liposomes is likely to be temperature dependent and so would be the contribution from oxygen broadening to A'. According to data reported by Windrem and Plachy (1980), the variation in P (and corresponding $\delta(A'(T))$ between 42°C and 51°C is less than 10% and therefore in our analysis $A'(T)$ can be considered to be constant at temperatures above the main phase transition. We anticipate the same small variations for $A'(T)$ in the temperature interval 32.5–40.0°C (ripple structure phase). We also found that the slope of the straight line in Fig. 10 does not change when only the points above the $P_{\beta'}$-L_α phase transition are taken into account. All this suggests that within the accuracy of our experiment the ratio A/B is constant for both ripple structure and fluid bilayer structure phases. (Other explanations are possible but less likely. The best approach would be to deoxygenate the LUV/TEMPO sample for these studies. We are currently working on a technique for deoxygenation of aqueous samples in 0.15-mm i.d. capillaries.) Therefore, the linear constraint imposed by the AVE equation remains the same for both $P_{\beta'}$ and L_α phases.

With the TEMPO magnetic parameters measured at 94.3 GHz (Table 1) and $A/B = 2.27$ (Fig. 10), the following AVE for TEMPO in the DPPC hydrocarbon phase was obtained:

$$\rho_x = 0.165\rho_y + 1.604 \quad (4)$$

Equation 4 is not consistent with the isotropic rotational diffusion of TEMPO in the hydrocarbon phase and is only consistent when the diffusion tensor is axially symmetric (when $\rho_x = \rho_y = \rho_\perp$ and $\rho_\parallel = 1$, then $\rho_\perp = 1.92$) or is fully anisotropic. One AVE equation cannot be used for the full determination of the diffusion tensor as it contains only one linear constraint for ρ_x and ρ_y. One way to set another constraint for ρ_x and ρ_y is to use ^{17}O substituted nitroxides (Kowert, 1981) or another EPR frequency (Budil et al., 1993). We have attempted to extract T_2 data from our 9.0-GHz experiment. As was discussed above, the fit of the low resolution 9.0-GHz spectra with all parameters adjusted as in the 94.3-GHz experiment was not unique (e.g., see Fig. 6). One possibility to reduce the number of adjustable parameters is to assume that at 9.0 GHz the line widths for all three nitrogen hyperfine components corresponding to the TEMPO signal in the aqueous phase are the same (at X-band and room temperature the line width contribution from the rotational motion of the TEMPO in water is negligible compared with broadening from unresolved proton superhyperfine and oxygen). With this model, the line widths for TEMPO in the membrane phase were extracted from the experimental spectra (Fig. 11). Fig. 11 demonstrates that at 9.0 GHz the overall changes in $T_2^{-1}(m_I)$ are rather small; only the high field component undergoes measurable changes. The average value for $T_2^{-1}(m_I = 0)$ is 0.425 G, which is close to the intersect $A' = 0.43 \pm 0.09$ G measured from the W-band experiment. Overall, the accuracy of $T_2^{-1}(m_I)$ extracted from the 9.0-GHz data seems to be insufficient to derive line width parameters

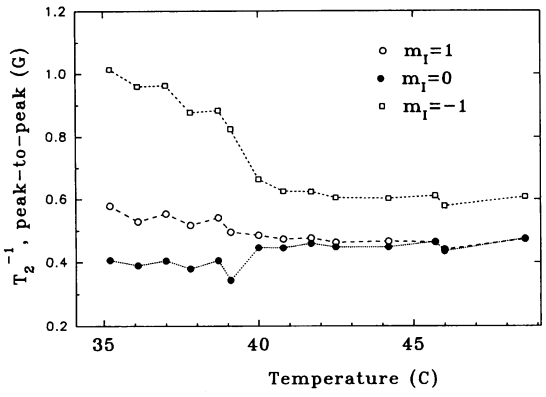

FIGURE 11 Temperature dependence of the homogeneous (Lorentzian) peak-to-peak line width for spectra of TEMPO in the hydrocarbon phase extarcted from 9.0-GHz (X-band) experiments. Nitrogen hyperfine components are numbered according to the nuclear quantum number m_I. In least-squares simulations the same line widths were assumed for all three nitrogen hyperfine components corresponding to the TEMPO signal in the aqueous phase (see text). The estimates of errors are approximately 10%.

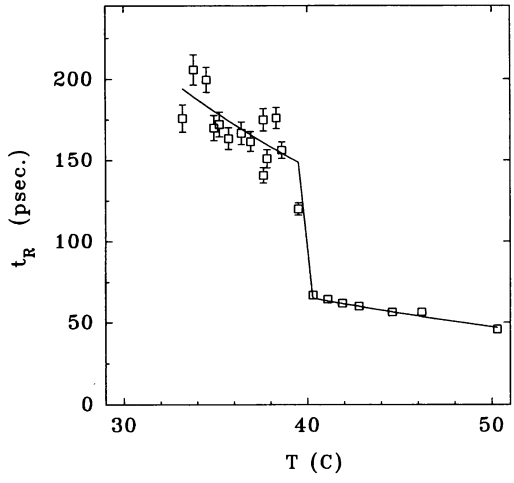

FIGURE 12 Temperature dependence of rotational correlation time τ_R calculated from the line width parameter B. The chosen anisotropy parameters $\rho_X = 1.86$ and $\rho_Y = 1.54$ satisfy the AVE calculated for $A/B = 2.27$. The solid line is the least-squares fit of the data points assuming different membrane fluidities for the ripple structure and the fluid bilayer structure phases of the LUVs.

for TEMPO at this frequency. The accuracy at 9.0 GHz could be significantly improved by applying specially designed deuterated nitroxides (e.g., see Seversan and Cannistraro, 1988, 1989). Unfortunately, at this moment, these nitroxides are not available to the authors.

Budil et al. (1993) determined the full diffusion tensor for the perdeuterated TEMPONE (2,2′,6,6′-tetramethyl-4-piperidine-1-nitroxide) nitroxyl radical in toluene-d_8 using data from 9.5 and 250 GHz ($\rho_x = 1.8 \pm 0.2$, $\rho_y = 1.5 \pm 0.3$). The molecular structure of the TEMPONE probe is very similar to the TEMPO used in our work (it differs only by one ketone oxygen on position 3 of the piperidine ring). If we assume that TEMPO has a similar but slightly larger rotation anisotropy, $\rho_x = 1.86$ and $\rho_y = 1.54$, these values will satisfy Eq. 4. Although we cannot determine the full diffusion tensor from the data obtained at one EPR frequency (W-band, 94.2 GHz), our data, including anisotropy parameters ρ_x and ρ_y, seems to be consistent with the full anisotropic Brownian diffusion model developed in Budil et al. (1993). Within the accuracy of our experiment at 94.3 GHz, we cannot see any measurable deviation from the isotropic Brownian diffusion model for the rotational diffusion of the TEMPO within the phospholipids ($P_{\beta'}$ and L_α phases). This also suggests that if in our experiment some ordering of the TEMPO in the lipid phase did exist, then its effect on the EPR spectra is small.

We have chosen the anisotropy parameters $\rho_x = 1.86$ and $\rho_y = 1.54$ to derive the TEMPO rotational correlation time τ_R using the τ_R definition given for a fully anisotropic case by Budil et al. (1993). Values of τ_R were calculated from the spectral parameter B, which is not affected by possible small variations in $A'(T)$. The plot of τ_R versus T and the least-squares fit for τ_R versus T is shown in Fig. 12. An abrupt decrease in τ_R between 40 and 41°C (corresponding to the main phase transition temperature) indicates an increase in the membrane fluidity at temperatures above the main phase transition of approximately a factor of two.

The results presented here demonstrate the advantages of VHF EPR in dynamic studies of nitroxide probes partitioning between aqueous and hydrocarbon phases. Unique information about the rotational diffusion tensor can be obtained together with accurate partitioning data. Within the accuracy of our experiment, for the motion of the TEMPO in the lipid phase, we cannot see any measurable deviations from the isotropic Brownian diffusion model. We anticipate that the use of our simulation and EPR partitioning data at various, but preferably >50 GHz, EPR frequencies will provide a set of AVE equations necessary for the full determination of the rotational diffusion tensor of the probe molecule in the membrane hydrocarbon phase. This information may be also helpful to further determine whether ordering of TEMPO can be always neglected in partitioning experiments or whether it must be included, and the degree to which ordering occurs. As some nitroxide radical probes can mimic drugs and other biologically important molecules, it is of interest to look at the dynamics of these probes in liposome membranes and to determine the effects of different substances on these dynamics. It appears that VHF EPR can be very helpful in providing such information.

We thank Prof. Belford (Chemistry Department, University of Illinois) for his interest in this work and useful suggestions.

The work used the resources of the Illinois EPR Research Center supported by National Institutes of Health grant RR01811. Elements of the software package and computer hardware used in this work were in part provided by Scientific Software Services (Bloomington, IL). PDM greatfully acknowledges support from the National Institutes of Health (1R15GM44365–01).

REFERENCES

Budil, D. E., K. A. Earle, and J. H. Freed. 1993. Full determination of the rotational diffusion tensor by electron paramagnetic resonance at 250 GHz. *J. Phys. Chem.* 97:1294–1303.

Chen, S. C., and J. M. Sturtevant. 1981. Thermotropic behavior of bilayers formed from mixed-chain phosphatidylcholines. *Biochemistry.* 20:713–718.

Costanzo, R., T. D. Paoli, J. E. Ihlo, A. A Hager, H. A. Farach, C. P. Poole, and J. M. Knight. 1994. ESR study of order and dynamics in lecithin liposomes with high cholesterol content. *Spectrochim. Acta.* 50A:203–208.

Crepeau, R. H., S. Saxena, S. Lee, B. Patyal, and J. K. Freed. 1994. Studies on lipid membranes by two-dimensional Fourier transform ESR: enhancement of resolution to ordering and dynamics. *Biophys. J.* 66:1489–1504.

Dalton, L. A., and K. W. Miller. 1993. *Trans*-unsaturated lipid dynamics: modulation of dielaidoylphosphatidylcholine acyl chain motion by ethanol. *Biophys. J.* 65:1–12.

Freed, J. H. 1964. Anisotropic rotational diffusion and electron spin resonance linewidths. *J. Chem. Phys.* 41:2077–2083.

Freed, J. H. 1987. Molecular rotational dynamics in isotropic and oriented fluids studied by ESR. *In* Rotational Dynamics of Small and Macromolecules in Liquids. T. Dorfmuller and R. Pecora, editors. Springer-Verlag, Berlin. 89–142.

Ge, M., and J. H. Freed. 1993. An electron spin resonance study of interactions between gramicidin A′ and phosphatidylcholine bilayers. *Biophys. J.* 65:2106–2123.

Grinberg, O. Y., A. A. Dadali, A. A. Dubinskii, A. M. Vasserman, A. L. Buchachenko, and Y. S. Lebedev. 1979. Determination of g and A tensor components and rotational mobility of nitroxide radicals by 2-mm EPR spectroscopy. *Teor. Eksp. Khim.* 15:583–588.

Halpern, H. J., M. Peric, C. Yu, and B. Bales. 1993. Rapid quantitation of parameters from inhomogeneously broadened EPR spectra. *J. Magn. Reson. A.* 103:13–22.

Keith, A. D., and W. Snipes. 1974. Viscosity of cellular protoplasm. *Science.* 183:66–668.

Kowert, B. A. 1981. Determination of the Anisotropic and nonsecular contributions to ESR line widths in liquids. *J. Phys. Chem.* 85:229–235.

Lee, A. G., N. J. M. Birdsall, J. C. Metcalfe, P. A. Toon, and G. B. Warren. 1974. Clusters in lipid bilayers and the interpretation of thermal effects in biological membranes. *Biochemistry.* 13:3699–3705.

Linden, C. D., K. L. Wright, H. M. McConnell, and C. F. Fox. 1973. Lateral phase separation in membrane lipids and the mechanism of sugar transport in *Escherichia coli. Proc. Natl. Acad. Sci. USA.* 70:2271–2275.

Mayer, L. D., M. J. Hope, and P. R. Cullis. 1986. Vesicles of variable sizes produced by a rapid extrusion procedure. *Biochim. Biophys. Acta.* 858: 161–168.

Meirovitch, E., and J. H. Freed. 1980. ESR studies of low water content 1,2-dipalmitoyl-*sn*- glycero-3-phosphocholine in oriented multilayers. I. Evidence for long-range cooperative chain distortions. *J. Phys. Chem.* 84:3281–3295.

Meirovitch, E., and J. H. Freed. 1980. ESR studies of low water content 1,2-dipalmitoyl-*sn*-glycero-3-phosphocholine in oriented multilayers. II. Evidence for magnetic-field-induced reorientation of the polar headgroups. *J. Phys. Chem.* 84:3295–3303.

Meirovitch, E., A. Nayeem, and J. H. Freed. 1984. Analysis of protein-lipid interactions based on model simulations of electron resonance spectra. *J. Phys. Chem.* 88:3454–3465.

Morimoto, Y., M. Hosokawa, H. Sayo, and Y. Takeuchi. 1994. ESR study of membrane perturbation and the lysis of liposomes induced by chlorpromazine. *Chem. Pharm. Bull.* 42:123–129.

Morse, P. D. II. 1977. Use of the spin label tempamine for measuring the internal viscosity of red blood cells. *Biochem. Biophys. Res. Commun.* 77:1486–1491.

Morse, P. D. II, R. L. Magin, and H. M. Swartz. 1985. Improved temperature control for samples in electron paramagnetic resonance spectroscopy. *Rev. Sci. Instrum.* 56:94–96.

Nordio, P. L. 1976. General magnetic resonance theory. *In* Spin Labeling: Theory and Applications. L. J. Berliner, editor. Academic Press, New York. 5–52.

Ondar, M. A., O. Y. Grinberg, A. A. Dubinskii, and Y. S. Lebedev. 1985. Study of the effect of the medium on the magnetic-resonance parameters of nitroxyl radicals by high-resolution EPR spectroscopy. *Sov. J. Chem. Phys.* 3:781–792.

Plachy, W. Z., and D. A. Windrem. 1977. A gas-permeable ESR sample tube. *J. Magn. Reson.* 27:237–239.

Polnaszek, C. F., S. Schreier, K. W. Butler, and I. C. P. Smith. 1978. Analysis of the factors determining the EPR spectra of spin probes that partition between aqueous and lipid phases. *J. Am. Chem. Soc.* 100:8223–8231.

Press, W. H., S. A. Teukolski, W. T. Vetterling, and B. P. Flannery. 1986. Numerical Recipes in Fortran, 2nd ed. Cambridge University Press, Cambridge, UK. 678–683.

Rothenberger, K. S., R. F. Sprecher, S. M. Castellano, and H. L. Retcofsky. 1993. Temperature dependence of the electron paramagnetic resonance intensity of whole coals: the search for triplet states. *In* Magnetic Resonance of Carbonaceous Solids. R. E. Botto and Y. Sanada, editors. American Chemical Society, Washington, DC. 581–604.

Schneider, D. J., and J. H. Freed. 1989. Calculation of slow motional magnetic resonance spectra: a user's guide. *In* Biological Magnetic Resonance, Vol 8. L. J. Berliner and J. Reuben, editors. Plenum Press, New York. 1–76.

Schreier, S., C. F. Polnaszek, and I. C. Smith. 1978. Spin label in membranes: problems in practice. *Biochim. Biophys. Acta.* 515:375–436.

Seelig, J. 1970. Spin label studies of oriented smectic liquid crystals (a model system for bilayer membranes). *J. Am. Chem. Soc.* 92:3881–3887.

Severcan, F., and S. Cannistraro. 1988. Use of PDDTBN spin probe in partition studies of lipid membranes. *Chem. Phys. Lett.* 153:263–267.

Severcan, F., and S. Cannistraro. 1989. Model membrane partition ESR study in the presence of α-tocopherol by a new spin probe. *Biosci. Rep.* 9:489–495.

Shimshick, E. J., and H. M. McConnell. 1973. Lateral phase separation in phospholipid membranes. *Biochemistry.* 12:2351–2360.

Smirnov, A. I., and R. L. Belford. 1995. Rapid quantitation from inhomogeneously broadened EPR spectra by a fast convolution algorithm. *J. Magn. Reson. A.* 113:65–73.

Smirnov, A. I., S. W. Norby, T. Walczak, K. J. Liu, and H. M. Swartz. 1994. Physical and instrumental considerations in the use of lithium phthalocyanine for measurements of the concentration of the oxygen. *J. Magn. Reson. B.* 103:95–102.

Subczynski, W. K., J. S. Hyde, and A. Kusumi. 1989. Oxygen permeability of phosphatidylcholine-cholesterol membranes. *Proc. Natl. Acad. Sci. USA.* 86:4474- 4478.

Wang, W., R. L. Belford, R. B. Clarkson, P. H. Davis, J. Forrer, M. J. Nilges, M. D. Timken, T. Walczak, M. C. Thurnauer, J. R. Norris, A. L. Morris, and Y. Zwang. 1994. Very high frequency EPR - 94 GHz instrument and applications to primary reaction centers from photosynthetic red bacteria and to other disordered systems. *Appl. Magn. Reson.* 6:195–215.

Wang, D.-C., T. F. Taraschi, E. Rubin, and N. Janes. 1993. Configuration entropy is the driving force of ethanol action on membrane architecture. *Biochim. Biophys. Acta.* 1145:141- 148.

Windrem, D. A., and W. Z. Plachy. 1980. The diffusion-solubility of oxygen in lipid bilayers. *Biochim. Biophys. Acta.* 600:655–665.

Wu, S. H., and H. M. McConnell. 1975. Phase separation in phospholipid membranes. *Biochemistry.* 14:847–854.